

# Infrasound signals from a ground-truth source and implications from atmospheric models: ARIANE engine tests in Southern Germany revisited

K. Koch & C. Pilger

Bundesanstalt für Geowissenschaften und Rohstoffe (BGR), Stilleweg 2, D-30655 Hannover, Germany, E-mail: karl.koch@bgr.de; christoph.pilger@bgr.de

## 1 Abstract

Over the past two decades the German Aerospace Center (DLR) facility near Heilbronn, Germany, has conducted a considerable number of tests of the ARIANE-5 main engine. Infrasound signals from many of these tests (~40%) have been observed at IMS station IS26 at a distance of about 320 km in an easterly direction (99° east-southeast from North). Due to the prevailing weather pattern in Central Europe, nearly all detected tests occurred during the winter months from October to April, when the stratospheric wind points in an eastern direction, while it reverses during the summer season. Except for a single event in May 2012, the summer months (May through September) did not yield any infrasound signal detections from the engine tests. On the other hand, not all tests conducted in winter are observed either, while detection in the spring and fall equinox months of April and October must be considered to occur incidentally.

The large database of about 160 engine tests enables us to assess how well propagation modelling based on a standard atmospheric specification such as the ECMWF forecast model conforms with observed detections and non-detections. While reversal of the stratospheric wind pattern in the summer season eliminates the stratospheric duct towards the eastern direction, the case of non-detections in the winter season may be of a more subtle nature. Besides increases in background noise levels due to heavy winds at the station, the fine structure of the stratospheric duct in the atmospheric model should determine the detection capability at IS26, which could be located inside or outside a shadow zone at a specific time. Ultimately, the standard atmospheric model used may not be an accurate description of the atmosphere in such cases either. This work on a controlled ground truth infrasound source will thus increase our understanding on the relationship between infrasound detection capabilities and atmospheric specifications over the seasons.

## 2 Geographic map and annual distribution of engine tests

Fig. 1: Location map

Geographical location of the testing site of DLR at Lampoldshausen near Heilbronn and IMS infrasound station IS26 in the Bavarian Forest. The distance between the ARIANE source and IS26 amounts to about 320 km and the backazimuth from IS26 is ~280° (solid line is for great circle path and arrow for direction). The locations of the following cities are as follows: F—Frankfurt S—Stuttgart M—Munich N—Nuremberg R—Regensburg PR—Prah HN—Heilbronn UL—Ulm A—Augsburg PA—Passau

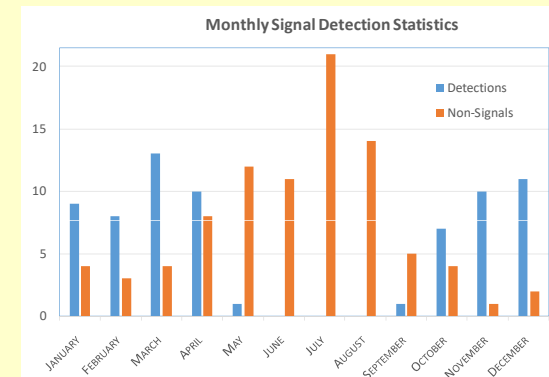
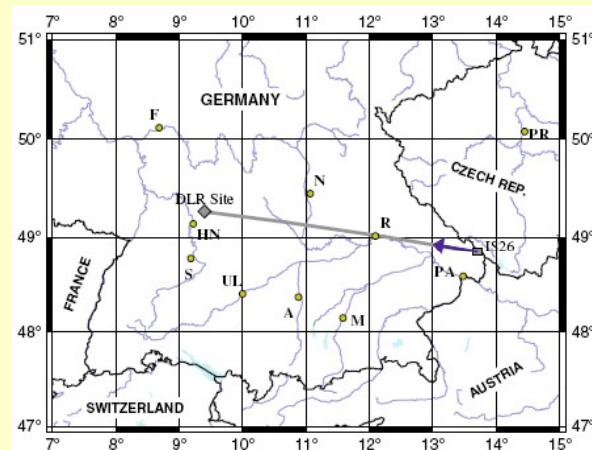


Fig. 2: Monthly statistics on observations (detections) and non-detections

Of the total number of 172 ARIANE engine tests 13 had durations of less than 10 seconds, with all of them not being observed, and thus were not included in the monthly statistics. Between November and April the majority of tests showed identifiable signals at IS26 (appropriate back azimuth from F-K analysis and duration from available ground truth information)

Table 1: Summary of monthly detection statistics

| Month | Det. | Non-Det. |
|-------|------|----------|
| Jan   | 9    | 4        |
| Feb   | 8    | 3        |
| Mar   | 13   | 4        |
| Apr   | 10   | 8        |
| May   | 1    | 12       |
| Jun   | 0    | 11       |
| Jul   | 0    | 21       |
| Aug   | 0    | 14       |
| Sep   | 1    | 5        |
| Oct   | 7    | 4        |
| Nov   | 10   | 1        |
| Dec   | 11   | 2        |
| Sum   | 70   | 89       |

## 3 Results from data processing and analysis

Relevant waveform observations from the ARIANE engine tests recorded at the infrasound array IS26 are identified based on two main criteria: (1) a signal of length corresponding to the propulsion duration (from ground truth) within a time window lagging the test's start time by about 15-16 minutes, and (2) array processing output with backazimuth near 280° and an acoustic trace velocity (or slowness on the order of 300-340 s/deg). In addition, we determined the RMS amplitude levels for signal-to-noise ratios (SNRs).

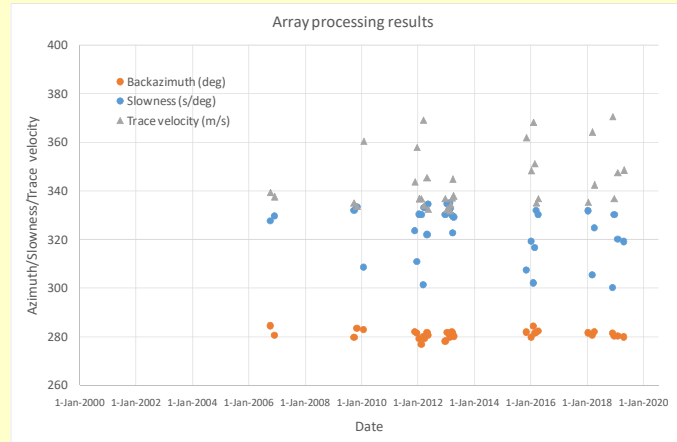
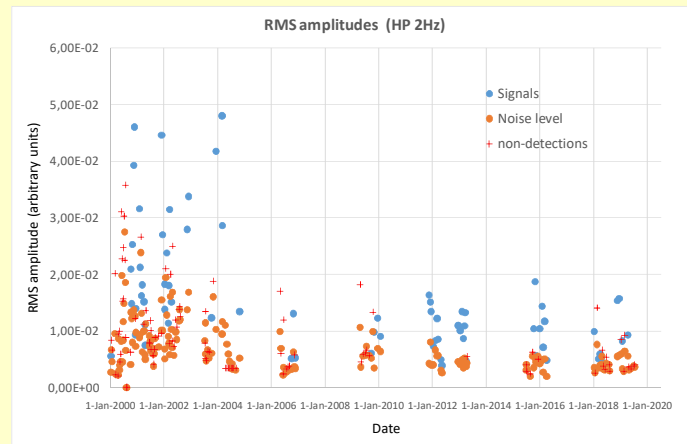


Fig. 3: Array processing results from frequency-wavenumber (F-K) analysis of signal observations since 2006. Estimated backazimuths (in degrees) are shown by yellow dots, slowness estimates (in s/deg) by blue dots, and slowness converted to trace/apparent velocity (in m/s) by gray triangles. Backazimuths show a small scatter within about ±3-5 degrees from the theoretical value, while slowness (or trace velocity, resp.) are more variable which may be an expression of changes in effective sound speeds. Results prior to 2006 are given by Koch (2010) and not reproduced here.

Fig. 4: Noise and signal levels for detections and non-detections.

For all ground truth events appropriate time windows for the background noise and the signals were chosen and RMS amplitude levels determined. Noise data are shown by yellow dots, while RMS values of signal observations (detections) are marked by blue dots. Waveform amplitude levels for non-detections are represented by red crosses. While non-detections mostly represent noise levels (i.e. SNR<1), except for disturbances, detections show SNRs up to 5. Note the general drop in signal levels starting in 2004 due to the installation of different impedance filters for wind noise reduction.



## 4 Effective source speed profiles comparison

For the 70 cases of signal detection and the 89 cases of non-detection we compared the corresponding effective sound speed profiles defined by the atmospheric specifications from the European Centre for Medium-Range Weather Forecast (ECMWF) to explain the observations. While for signal detections normally a stratospheric duct is found, it is mostly absent for non-detections.

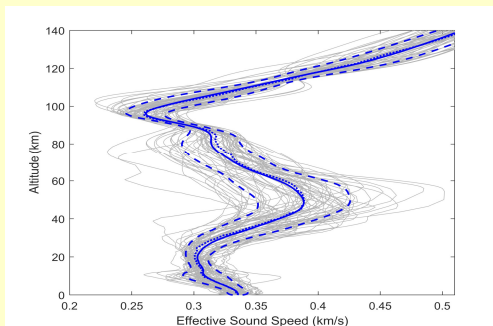


Fig. 5: Sound speed profiles for the cases of signal detection. The sound speed profiles in the case of signals detections clearly show a stratospheric duct that is observed within one standard deviation (dashed lines) of the mean (solid line). The median (dotted line) and mean curves match well.

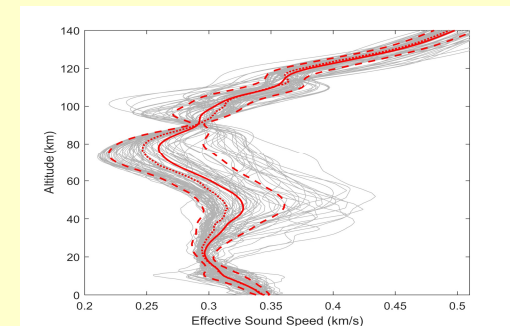


Fig. 6: Sound speed profiles for the cases of lacking signals. When no signal detections occur, sound speed profiles are mostly characterized by the lack of a stratospheric duct. Cases with a stratospheric duct are work in progress (not yet examined in details). Note the discrepancy between median and mean.

## 5 Examination of selected cases with signals

Following from Fig. 2 engine tests between the months of November to April are mostly detected at IS26, while in other months they are not. From Figs. 5 and 6 it is seen that effective sound speed profiles for detections consistently exhibit stratospheric ducts, and this is different for the majority of cases with non-detections. Here we examine two cases of detections in late 2018 (just before a SSW episode began) and we investigate the results from 2D parabolic equation modeling calculations. Similar modeling will be conducted in future work, especially for cases with favorable propagation conditions but without an identifiable signal, and eventually compared to signal-to-noise ratios (see Fig.4).

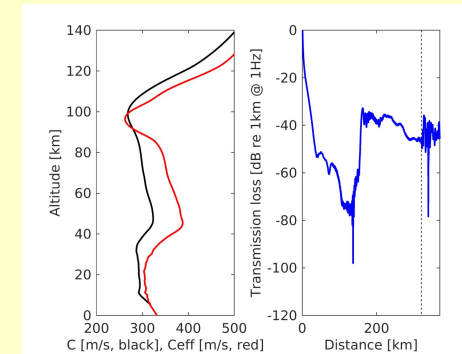


Fig. 7: Sound speed profile and amplitude pattern at surface level for Nov. 28, 2018.

Effective sound speeds clearly exhibit a stratospheric duct for favorable propagation towards IS26 (dashed line). Shallow tropospheric sound speeds (0-10-20km) were adjusted to omit, or at least reduce, the local winds at these altitudes.

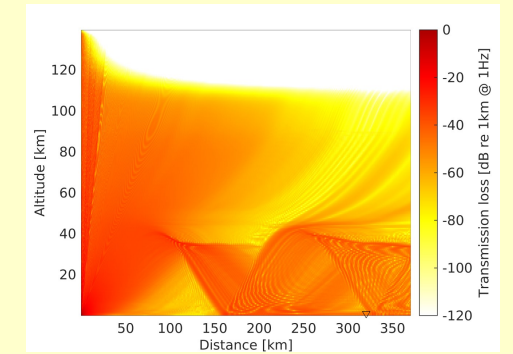


Fig. 8: Propagation pattern from 2D-PE calculations for Nov. 28, 2018.

Propagation in the direction of IS26 (symbolized by triangle) shows a first bounce point near 150 km and the second one near the station. The amplitude pattern in Fig. 7 reflects this as well, with an amplitude loss on the order of 40dB.

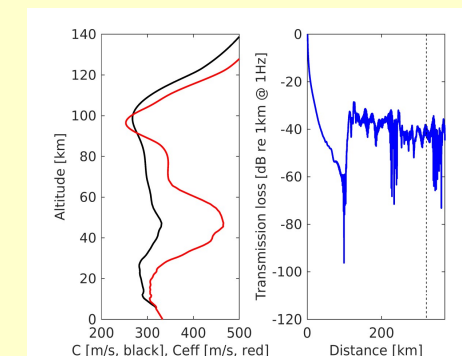


Fig. 9: Same as Fig. 7 for a test on Dec. 18, 2018.

The effective sound speed has an even more pronounced stratospheric duct with an effective sound speed ratio significantly larger than 1. Tropospheric sound speeds (0-10-20km) adjusted as before.

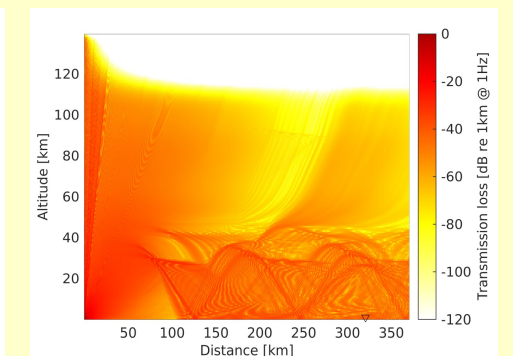


Fig. 10: Same as Fig. 8 for a test on Dec. 18, 2018.

Propagation modelling towards IS26 displays a more evenly spread energy pattern beyond about 100 km (first bounce) that is also revealed in the amplitude decay with distance to about 40dB at 320 km (Fig. 9).

## 6 Summary and conclusions

- Of the ARIANE5 engine tests carried out in the two decades since the year 2000, more than 40% produced detectable signals at IS26 at 320 km distance to the east-southeast.
- Except for one in May, one in September and four in October, all detected tests were done in the winter season from November to April, confirming previous results (see Koch, 2010; Pilger et al., 2013). In contrast, all tests between June and August and most in May, September and October were missed, even though noise levels were fairly stable.
- Detections and non-detections at IS26 are clearly related to changes in effective sound speed caused by the reversal of stratospheric wind patterns near the fall and spring equinoxes.
- Future work will investigate in greater detail the lack of signals when the effective sound speed profile seems favorable for infrasound propagation, but resulted in a non-detection potentially related to stratospheric shadow zones.

Ref: Koch, K. (2010). Analysis of Signals from an Unique Ground-Truth Infrasound Source Observed at IMS Station IS26 in Southern Germany. Pure Appl. Geophys., 167, 401-412, DOI 10.1007/s00024-009-0031-2.  
Pilger, C., F. Streicher, L. Ceranna & K. Koch (2013). Application of Propagation Modeling to Verify and Discriminate Ground-Truth Infrasound Signals at Regional Distances, Inframat. 2, 39-55, DOI 10.4236/inframat.2013.24004